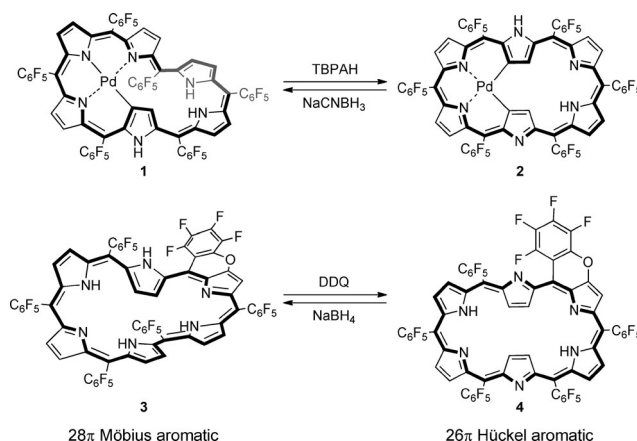


A Möbius Antiaromatic Complex as a Kinetically Controlled Product in Phosphorus Insertion to a [32]Heptaphyrin**

Tomohiro Higashino, Byung Sun Lee, Jong Min Lim, Dongho Kim,* and Atsuhiko Osuka*

In recent years, the π -conjugation topology has become an important issue in discussing aromaticity of organic molecules, since quite a number of Möbius aromatic molecules have been actually explored in which the $[4n]\pi$ -electronic macrocyclic conjugation is attained along a singly twisted one-sided topology like a Möbius strip (so-called Möbius topology).^[1] The concept of Möbius aromaticity first proposed by Heilbronner in 1964 is complementary to the usual Hückel aromaticity by predicting that the $[4n]\pi$ and $[4n+2]\pi$ rule for aromaticity of the usual two-sided topology (so-called Hückel topology) should be reversed for macrocyclic molecules of Möbius topology.^[2] *meso*-Aryl expanded porphyrins have emerged as an effective platform to realize Möbius aromatic systems owing to their conjugated nature, conformational flexibilities, and facile capture and release of two pyrrolic protons upon two-electron oxidation and reduction, respectively.^[3]

Despite the increasing number of $[4n]\pi$ Möbius aromatic molecules, $[4n+2]\pi$ Möbius antiaromatic molecules are still very rare.^[4,5] This is not surprising, as Möbius antiaromatic molecules should be unfavorable both from electronic and structural standpoints. As a rare example, Latos-Grażyński et al. reported a cationic palladium(II) complex of [18]vacataporphyrin that exhibited a weak paratropic ring current.^[4a] We have explored a bis(phosphorus) complex of [30]hexaphyrin, which is, to the best of our knowledge, the only example of a structurally well-characterized Möbius antiaromatic molecule.^[4b] As shown in Scheme 1, our previous attempts to form Möbius antiaromatic [26]hexaphyrins by the oxidations of Möbius aromatic [28]hexaphyrins **1** and **3** failed, merely producing Hückel aromatic [26]hexaphyrins **2** and **4** by a topology switch without detection of putative Möbius antiaromatic [26]hexaphyrins.^[3f,g] Herein, we report that



Scheme 1. Attempts at forming Möbius antiaromatic species. TBPAH = tris(4-bromophenyl)aminium hexachloroantimonate, DDQ = 2,3-dichloro-5,6-dicyano-1,4-benzoquinone.

phosphorus insertion to [32]heptaphyrin **7** led to the formation of a Möbius antiaromatic phosphorus complex of [34]heptaphyrin, **8**, as a kinetically controlled product, which thermally rearranged to a more stable Hückel aromatic complex **9** quantitatively.

meso-Aryl-substituted heptaphyrins(1.1.1.1.1.1.1) usually take 32π oxidation states as the most stable forms. Our studies on the phosphorus insertion into *meso*-aryl expanded porphyrins have revealed that the coordinated phosphorus atoms exist as a P^V state either in a phosphoramidate or five-coordinate form, stabilizing reduced oxidation states of expanded porphyrins.^[4b,6] We thus envisioned that [34]heptaphyrins may be generated by the phosphorus insertion into heptaphyrins, while such reduced heptaphyrins have the exception to the rule to date apart from a quadruply *N*-fused heptaphyrin.^[7]

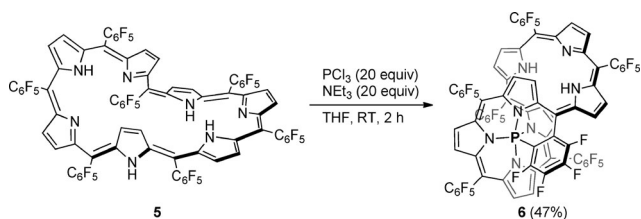
Initially, we attempted the phosphorus insertion into *meso*-pentafluorophenyl-substituted [32]heptaphyrin(1.1.1.1.1.1.1) **5**, which is known to display distinct Möbius aromaticity in polar solvents.^[3e,h] Treatment of **5** with PCl_3 in the presence of triethylamine in THF gave phosphorus complex **6** in 47% yield (Scheme 2). The high-resolution electrospray ionization time-of-flight (HR-ESI-TOF) mass spectrum of **6** displays a parent negative ion peak at $m/z = 1714.0556$ (calcd for $C_{77}H_{15}F_{34}N_7P$, $[M-H]^-$: 1714.0589), indicating the insertion of a phosphorus atom and elimination of a fluoride ion. The structure of **6** has been revealed by X-ray diffraction analysis to be a doubly twisted figure-of-eight (Hückel) conformation (Figure 1).^[8a] The phosphorus atom is five-coordinate, being bound to the four nitrogen atoms of the pyrrole A, B, C, and D, and the *ortho*-carbon atom of one of

[*] T. Higashino, Prof. Dr. A. Osuka
Department of Chemistry, Graduate School of Science
Kyoto University, Sakyo-ku, Kyoto, 606-8502 (Japan)
E-mail: osuka@kuchem.kyoto-u.ac.jp

B. S. Lee, J. M. Lim, Prof. Dr. D. Kim
Spectroscopy Laboratory for Functional π -Electronic Systems and
Department of Chemistry, Yonsei University
Seoul 120-749 (Korea)
E-mail: dongho@yonsei.ac.kr

[**] This work was supported by Grants-in-Aid (No. 22245006 (A) and 20108001 "pi-Space") for Scientific Research from MEXT. T.H. acknowledges a JSPS Fellowship for Young Scientists. The work at Seoul was supported by the Midcareer Researcher Program (2010-0029668) and World Class University (R32-2010-000-10217-0) Programs of MEST of Korea.

Supporting information for this article is available on the WWW under <http://dx.doi.org/10.1002/ange.201208147>.



Scheme 2. Synthesis of phosphorus complex **6**.

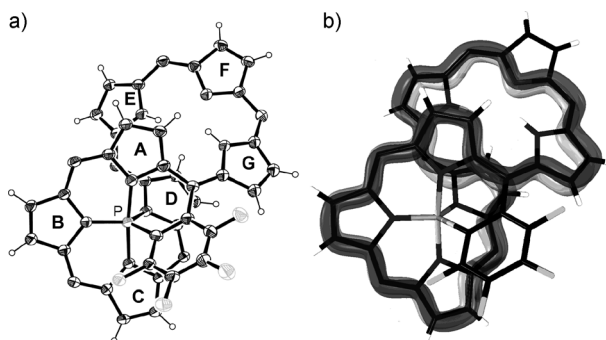
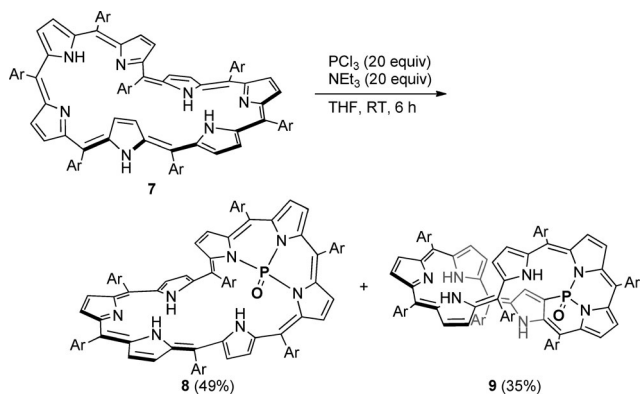


Figure 1. a) X-ray crystal structure of **6**. Ellipsoids are set at 30% probability. b) Representation of the molecular orbital of **6**. *meso*-Aryl substituents and solvent molecules in (a) and (b) have been omitted for clarity.

the *meso*-pentafluorophenyl groups in a trigonal bipyramidal manner. The ^1H NMR spectrum exhibits two signals at 13.73 and 13.61 ppm that are due to the NH protons and fourteen signals in the range of 8.08–5.07 ppm that are due to the pyrrolic β -protons. The ^{31}P NMR shows a signal at -82.41 ppm, which is in the range of five-coordinate phosphorus atoms with the same coordination geometry.^[6a,9] Complex **6** can be regarded as a weakly Hückel aromatic molecule, which is supported by its absorption characteristics.

In the next step, we examined the phosphorus insertion into *meso*-(2,6-dichlorophenyl)-substituted [32]heptaphyrin(1.1.1.1.1.1.1) **7** that is known to take a twisted Möbius structure even in nonpolar solvents.^[3c] Under similar conditions, treatment of **7** with PCl_3 gave two phosphorus complexes **8** and **9** in 49 and 35% yields, respectively (Scheme 3). The HR-ESI-TOF mass spectrum of **8** has



Scheme 3. Synthesis of phosphorus complexes **8** and **9**. Ar = 2,6-dichlorophenyl.

a parent positive ion peak at $m/z = 1603.8561$ (calcd for $\text{C}_{77}\text{H}_{39}\text{Cl}_{14}\text{N}_7\text{PO}$, $[\text{M}+\text{H}]^+$: 1603.8521). The structure of **8** has been revealed by X-ray diffraction analysis. Notably, complex **8** has a twisted Möbius conformation with a large dihedral angle (77°), in which the $\text{P}=\text{O}$ moiety is bound to the three nitrogen atoms of the pyrroles A, B, and C (Figure 2a).^[8b]

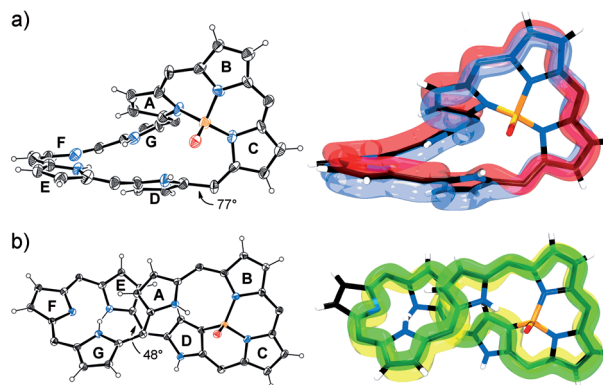


Figure 2. X-ray crystal structures (left) and representations of the molecular orbital (right) of a) **8** and b) **9**. Ellipsoids are set at 30% probability. *meso*-Aryl substituents and solvent molecules are omitted for clarity. Dihedral angles at the most distorted sites are indicated.

This structure, combined with its 34π -electronic network, tempted us to regard this as a Möbius antiaromatic molecule. This is indeed the case, as 1) the UV/Vis absorption spectrum of **8** has an ill-defined Soret-like band and weak and broad bands in near-IR region, which are characteristic of antiaromatic expanded porphyrins (Figure 3c);^[4b,10] and 2) the ^1H NMR spectrum of **8** characteristically displays signals

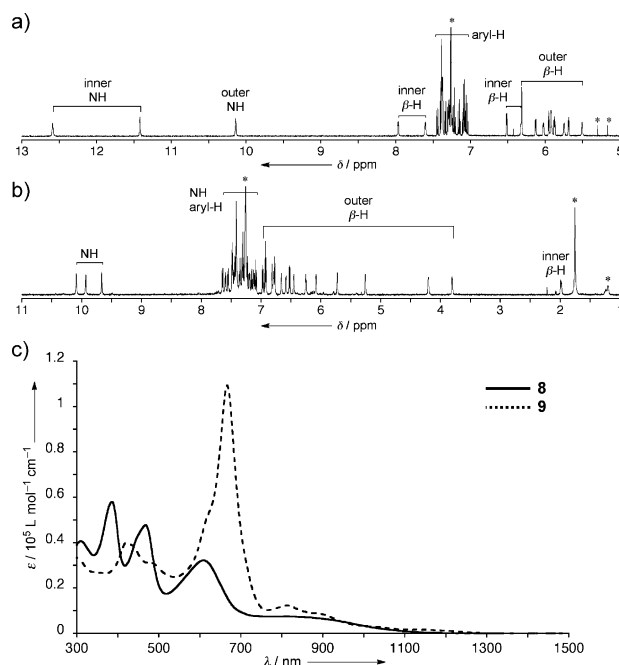
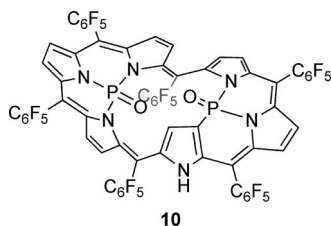


Figure 3. ^1H NMR spectra of a) **8** at 25°C and b) **9** at -60°C in CDCl_3 . Peaks marked with * arise from residual solvents and impurities. c) UV/Vis absorption spectra of **8** and **9** in CH_2Cl_2 .

owing to the inner (almost lateral) pyrrolic β -protons in the pyrrole rings A and D at 7.96 and 7.60 ppm, which are distinctly deshielded from the other outer β -protons that appear in the range of 6.51–5.51 ppm (Figure 3a), indicating a weak paratropic ring current. In line with this, the inner NH protons in the pyrroles E and G appear at 12.59 and 11.42 ppm, which are also deshielded relative to the outer one in the pyrrole D at 10.14 ppm. The difference between the chemical shifts of the most shielded and most deshielded β -protons ($\Delta\delta = \delta_{\text{outer}} - \delta_{\text{inner}}$) is only -2.45 ppm. The weaker paratropic ring current of **8** compared with that of Möbius antiaromatic phosphorus complex of [30]hexaphyrin **10** ($\Delta\delta$ is



-5.60 ppm and the largest dihedral angle is 67°)^[4b] can be ascribed to the larger dihedral angle.

The other complex **9** has been determined to take a doubly twisted figure-of-eight (Hückel) structure on the basis of X-ray diffraction analysis (Figure 2b).^[8c] The P=O moiety is bound to the two nitrogen atoms of the pyrroles B and C, and the β -carbon atom of the pyrrole D. Complex **9** has been assigned as a 34π -Hückel aromatic molecule. The UV/Vis absorption spectrum of **9** exhibits an intense Soret-like band at 667 nm and Q-band like bands at 813, 892, and 1157 nm (Figure 3c), which are characteristic of the aromatic porphyrinoids.^[10] The ^1H NMR spectrum of **9** is very broad at room temperature, which is probably due to conformational flexibility, but became sharpened at -60°C , exhibiting a doublet at 1.98 ppm owing to the inner β -proton in the pyrrole D adjacent to the P=O moiety and twelve signals owing to the other β -protons in a range of 6.91–3.80 ppm (Figure 3b). The chemical shift difference ($\Delta\delta$) is relatively large ($+4.93$ ppm), indicating the presence of a certain diatropic ring current.

The electrochemical properties were studied by cyclic voltammetry in CH_2Cl_2 versus ferrocene/ferrocenium ion (Fc/Fc^+) with tetrabutylammonium hexafluorophosphate as an electrolyte (see the Supporting Information). Complex **8** underwent two reversible reductions at -1.55 and -1.92 V and two reversible oxidations at -0.17 and 0.07 V, while complex **9** showed one reduction wave at -1.89 V and two oxidation waves at -0.34 and 0.08 V; all of these are reversible processes. The electrochemical HOMO–LUMO gaps were thus calculated to be 1.38 and 1.55 eV for **8** and **9**, respectively. The smaller HOMO–LUMO gap of **8** is consistent with its assignment as an antiaromatic species.

It has been established that excited-state properties of porphyrinoids can be used to evaluate the aromaticity.^[11] Typically, the transient absorption spectra of aromatic expanded porphyrins show strong ground-state bleaching

(GSB) signals with relatively weak excited-state absorption (ESA) signals. These aromatic signals were seen in the transient absorption spectra of **9** (Figure 4b), while those of **8**

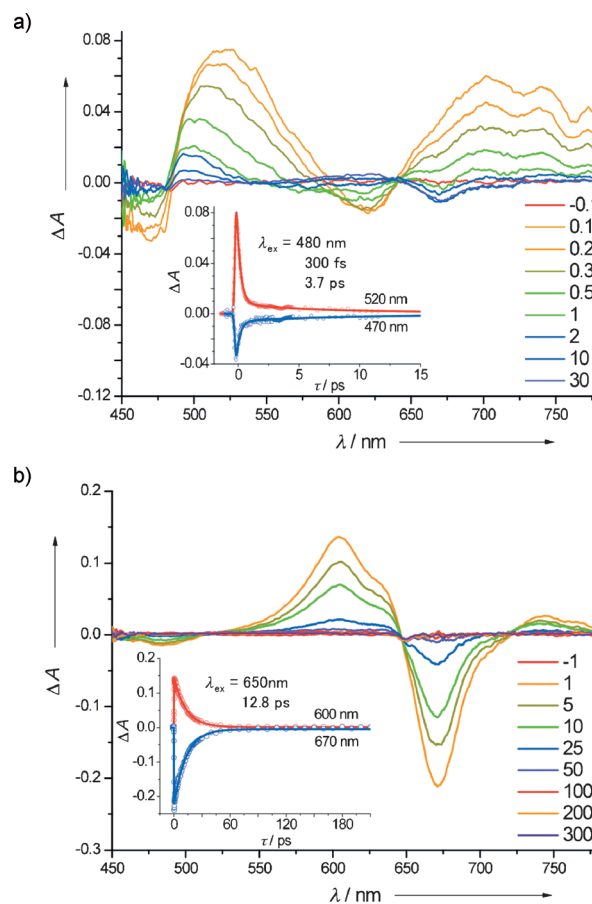


Figure 4. Transient absorption spectra of a) **8** and b) **9** at room temperature in toluene. The insets show the decay profiles.

showed the opposite trend, namely small GSB and large ESA signals. These spectral features, together with the faster decay dynamics of **8** (300 fs, 3.7 ps) than of **9** (12.8 ps), are characteristic for antiaromatic expanded porphyrins. The observed fast decay of **8** can be ascribed to the NIR dark state that acts as a ladder in the deactivation processes. The two-photon absorption (TPA) cross-section values of **8** and **9** were also measured by the wavelength-scanning open-aperture Z-scan method in the wavelength ranges of 1300–1900 nm, where the contribution of one-photon absorption is negligible. Möbius antiaromatic compound **8** exhibited relatively small TPA cross section of 1600 GM, which was nearly half of the TPA value of Hückel aromatic compound **9** (2800 GM). These data support the antiaromatic and aromatic characters for **8** and **9**, respectively.^[11a]

To obtain additional information on **8** and **9**, we performed theoretical calculation at RB3LYP/6-31G(d) level on the basis of the optimized structures by the Gaussian program (see the Supporting Information).^[12] Importantly, the total energy of **8** has been calculated to be higher by 31.0 kcal mol⁻¹ than that of **9**. Time-dependent DFT calculation predicts

a weak absorption band around 1037 nm for **8** and an intense Soret-like band at 630 nm for **9**, which are characteristic features of antiaromatic and aromatic expanded porphyrins, respectively.^[10]

Interestingly, the yields of **8** and **9** were found to be temperature-dependent, namely 33 and 17% with the recovery of **7** (45%) in the reaction at 0°C for 3 h and 18 and 74% at 60°C for 3 h. More directly, we examined the thermal conversion of **8** to **9** that involved the phosphoramidate rearrangement with a topology change from Möbius to Hückel. While rather stable toward heating at 60°C in THF, CHCl₃, and acetone, heating of **8** in acetonitrile at 60°C for 12 h gave rise to the quantitative transformation to **9**. These changes were clearly traced by UV/Vis spectroscopy (Supporting Information), and the rate of this conversion were determined by monitoring the increasing absorbance of **9** at 622 nm at various temperature to be $2.2 \times 10^{-6} \text{ s}^{-1}$ at 60°C, $3.9 \times 10^{-6} \text{ s}^{-1}$ at 65°C, $4.6 \times 10^{-6} \text{ s}^{-1}$ at 70°C, $5.9 \times 10^{-6} \text{ s}^{-1}$ at 75°C, and $9.3 \times 10^{-6} \text{ s}^{-1}$ at 80°C. On the basis of these results, the activation parameters of the rearrangement have been determined as follows: activation energy $E_a = 65.3 \text{ kJ mol}^{-1}$, activation enthalpy $\Delta H^\ddagger = 62.4 \text{ kJ mol}^{-1}$, and activation entropy $\Delta S^\ddagger = -166 \text{ J mol}^{-1}$ (See the Supporting Information). Thus, these results indicate that **8** is a kinetically controlled product that undergoes exothermic conversion into **9**. Curiously, this rearrangement proceeded in propionitrile and butyronitrile but not in benzonitrile, suggesting a specific role of aliphatic nitrile group in the rearrangement.

In summary, singly twisted Möbius antiaromatic [34]heptaphyrin **8** and doubly twisted Hückel aromatic [34]heptaphyrin **9** were formed in the phosphorus insertion reaction to [32]heptaphyrin **7**. The Möbius antiaromatic character of **8** has been confirmed on the basis of its X-ray structure, a weak paratropic ring current, ill-defined absorption characteristics, fast excited-state decay, and a relatively small TPA cross-section. In aliphatic nitrile solutions, complex **8** underwent the quantitative thermal migration of the P=O moiety to produce more stable **9** with the concurrent molecular topology switch, thus indicating the complex **8** to be a rare case of a kinetically controlled Möbius antiaromatic species.

Received: October 10, 2012

Published online: November 19, 2012

Keywords: aromaticity · heptaphyrins · Möbius antiaromaticity · phosphorus · porphyrinoids

- [1] a) H. E. Zimmerman, *Acc. Chem. Res.* **1971**, *4*, 272–280; b) H. S. Rzepa, *Chem. Rev.* **2005**, *105*, 3697–3715; c) R. Herges, *Chem. Rev.* **2006**, *106*, 4820–4842.
- [2] E. Heilbronner, *Tetrahedron Lett.* **1964**, *5*, 1923–1928.
- [3] a) M. Stępień, L. Latos-Grażyński, N. Sprutta, P. Chwalisz, L. Szterenberg, *Angew. Chem.* **2007**, *119*, 8015–8019; *Angew. Chem. Int. Ed.* **2007**, *46*, 7869–7873; b) Z. S. Yoon, A. Osuka, D. Kim, *Nat. Chem.* **2009**, *1*, 113–122; c) Y. Tanaka, S. Saito, S.

- Mori, N. Aratani, H. Shinokubo, N. Shibata, Y. Higuchi, Z. S. Yoon, K. S. Kim, S. B. Noh, J. K. Park, D. Kim, A. Osuka, *Angew. Chem.* **2008**, *120*, 693–696; *Angew. Chem. Int. Ed.* **2008**, *47*, 681–684; d) J. Sankar, S. Mori, S. Saito, H. Rath, M. Suzuki, Y. Inokuma, H. Shinokubo, K. S. Kim, Z. S. Yoon, J.-Y. Shin, J. M. Lim, Y. Matsuzaki, O. Matsushita, A. Muranaka, N. Kobayashi, D. Kim, A. Osuka, *J. Am. Chem. Soc.* **2008**, *130*, 13568–13579; e) S. Saito, J.-Y. Shin, J. M. Lim, K. S. Kim, D. Kim, A. Osuka, *Angew. Chem.* **2008**, *120*, 9803–9806; *Angew. Chem. Int. Ed.* **2008**, *47*, 9657–9660; f) S. Tokuji, J.-Y. Shin, K. S. Kim, J. M. Lim, K. Youfu, S. Saito, D. Kim, A. Osuka, *J. Am. Chem. Soc.* **2009**, *131*, 7240–7241; g) M. Inoue, A. Osuka, *Angew. Chem.* **2010**, *122*, 9678–9681; *Angew. Chem. Int. Ed.* **2010**, *49*, 9488–9491; h) M.-C. Yoon, J.-Y. Shin, J. M. Lim, S. Saito, T. Yoneda, A. Osuka, D. Kim, *Chem. Eur. J.* **2011**, *17*, 6707–6715.
- [4] a) E. Pacholska-Dudziak, J. Skonieczny, M. Pawlicki, L. Szterenberg, Z. Ciunik, L. Latos-Grażyński, *J. Am. Chem. Soc.* **2008**, *130*, 6182–6195; b) T. Higashino, J. M. Lim, T. Miura, S. Saito, J.-Y. Shin, D. Kim, A. Osuka, *Angew. Chem.* **2010**, *122*, 5070–5074; *Angew. Chem. Int. Ed.* **2010**, *49*, 4950–4954.
- [5] For a theoretical investigation of Möbius antiaromatic species in transition state of isomerization of annulenes, see: a) P. M. Warner, *J. Org. Chem.* **2006**, *71*, 9271–9282; b) J. F. Moll, R. P. Pemberton, M. G. Gutierrez, C. Castro, W. L. Karney, *J. Am. Chem. Soc.* **2007**, *129*, 274–275.
- [6] a) T. Miura, T. Higashino, S. Saito, A. Osuka, *Chem. Eur. J.* **2010**, *16*, 55–59; b) T. Higashino, A. Osuka, *Chem. Sci.* **2012**, *3*, 103–107.
- [7] S. Saito, A. Osuka, *Chem. Eur. J.* **2006**, *12*, 9095–9102.
- [8] a) Crystallographic data for **6**: C₇₇H₁₆F₃₄N₇P·4.5CH₃CN, $M_r = 1899.17$; monoclinic, space group $P2_1/a$ (No.14), $a = 23.9273(4)$, $b = 14.4256(3)$, $c = 25.0687(5)$ Å; $\beta = 117.3853(8)^\circ$; $V = 7682.6(3)$ Å³; $\rho_{\text{calcd}} = 1.642 \text{ g cm}^{-3}$; $Z = 4$; $R_1 = 0.0649$ [$I > 2.0\sigma(I)$], $wR_2 = 0.2095$ (all data), GOF = 1.054; b) Crystallographic data for **8**: C₇₇H₃₈Cl₁₄N₇OP·3(C₆H₄Cl₂), $M_r = 2045.39$; monoclinic, space group $P2_1/a$ (No.14), $a = 13.3585(3)$, $b = 36.8516(9)$, $c = 18.6890(5)$ Å; $\beta = 106.7185(13)^\circ$; $V = 8811.4(4)$ Å³; $\rho_{\text{calcd}} = 1.542 \text{ g cm}^{-3}$; $Z = 4$; $R_1 = 0.1140$ [$I > 2.0\sigma(I)$], $wR_2 = 0.3402$ (all data), GOF = 1.092; c) Crystallographic data for **9**: C₇₇H₃₈Cl₁₄N₇OP·4.5CH₃CN, $M_r = 1787.65$; monoclinic; space group $C2/c$ (No.15), $a = 55.0034(10)$, $b = 13.2978(2)$, $c = 23.9021(4)$ Å; $\beta = 112.7130(7)^\circ$; $V = 16126.8(5)$ Å³; $\rho_{\text{calcd}} = 1.473 \text{ g cm}^{-3}$; $Z = 8$; $R_1 = 0.0669$ [$I > 2.0\sigma(I)$], $wR_2 = 0.1809$ (all data), GOF = 1.037. CCDC 899880 (**6**), 899879 (**8**), and 899878 (**9**) contain the supplementary crystallographic data for this paper. These data can be obtained free of charge from The Cambridge Crystallographic Data Centre via www.ccdc.cam.ac.uk/data_request/cif.
- [9] D. B. Chesnut, L. D. Quin, *Tetrahedron* **2005**, *61*, 12343–12349.
- [10] a) S. Saito, A. Osuka, *Angew. Chem.* **2011**, *123*, 4432–4464; *Angew. Chem. Int. Ed.* **2011**, *50*, 4342–4373; b) S. Saito, A. Osuka, *Chem. Commun.* **2011**, *47*, 4330–4339.
- [11] a) S. Mori, K. S. Kim, Z. S. Yoon, S. B. Noh, D. Kim, A. Osuka, *J. Am. Chem. Soc.* **2007**, *129*, 11344–11345; b) M.-C. Yoon, S. Cho, M. Suzuki, A. Osuka, D. Kim, *J. Am. Chem. Soc.* **2009**, *131*, 7360–7367; c) J. M. Lim, Z. S. Yoon, J.-Y. Shin, K. S. Kim, M.-C. Yoon, D. Kim, *Chem. Commun.* **2009**, 261–273; d) J.-Y. Shin, K. S. Kim, M.-C. Yoon, J. M. Lim, Z. S. Yoon, A. Osuka, D. Kim, *Chem. Soc. Rev.* **2010**, *39*, 2751–2767.
- [12] M. J. Frisch, et al., *Gaussian09*, revision A.02; Gaussian, Inc.: Wallingford, CT, **2009**.